

Improving the electrical conductivity and photo-conductivity of the photo-active layer P3HT:PCBM doped by Schiffbase for organic photo-sensor applications

Furat A Al-Saymari¹, Sundes J Fakher¹, Fadhil A Tuma¹, Raed A Alharis²,
Jasim M S Alshawi², M A Mahdi³, Imad Al-Deen H A Al-Saidi^{1,4} and
Qusay M A Hassan¹

¹ Department of Physics, College of Education for Pure science, University of Basrah, Basrah, Iraq

² Department of Chemistry, College of Education for Pure science, University of Basrah, Basrah, Iraq

³ Department of Physics, College of science, University of Basrah, Basrah, Iraq

⁴ Department of Computer Technology Engineering, Al-Kunooze University College, Basrah, Iraq

E-mail: qusayali64@yahoo.co.in

Received 10 April 2024

Accepted for publication 15 December 2024

Published 7 January 2025



CrossMark

Abstract

A Schiff-base material was synthesized and characterized by the ¹H- and ¹³C-NMR, FTIR, Mass, and UV-visible spectroscopy. A thin layer of pure P3HT:PCBM and P3HT:PCBM:Schiffbase with two concentrations 2 mM and 4 mM are prepared using spin coating method. At room temperature, doping of P3HT:PCBM active-layer by Schiff-base material at concentration of 4 mM led to enhance the electrical current and conductivity by a factor of 24x under dark conditions and by a factor of 27x under white-light illumination ($I_0 = 50 \text{ mW cm}^{-2}$). The electrical current, conductivity, and resistivity are measured as a function of time under illumination for three different wavelengths, white, green, and red, proving that the photo-sensors based on P3HT:PCBM:schiffbase thin films exhibit a good reproducibility, fast-response time, and high optical-sensitivity. It was also found that the photo-electrical characterization of the photo-sensors are wavelength dependent, where, under red-light, the samples exhibit the lowest optical-response while the highest value was obtained under white-light. The study revealed that the photo-responsivity and quantum efficiency of the P3HT:PCBM:Schiffbase (4 mM) based photo-sensors exposed by white light are higher than those the corresponding values of the photo-sensors based on P3HT:PCBM by a factor of $\sim 31x$. Moreover, the performance of the photo-sensors were improved due to depositing an ultra-thin film of carbon on top of the active-layer, exhibiting a significant enhancement in the electrical and photo-electrical properties. The photo-sensors based on P3HT:PCBM:Schiffbase/carbon-nano-sheet show a superior quantum efficiency ($\sim 6\%$) with photo-responsivity of $\sim 24 \text{ mA W}^{-1}$, confirming that the doped P3HT:PCBM active-layer are very interesting for organic optical sensors and photovoltaic devices.

Supplementary material for this article is available [online](#)

Keywords: organic semiconductor, P3HT:PCBM active layer, photo-conductivity, Schiffbase material, organic photo-sensors

Classification numbers: 4.10, 5.03

1. Introduction

The polymer blends materials have emerged as a class of optoelectronic and electronic media for both experimental and theoretical considerations. They present a special interest of light weight, low cost technologies, ease of processing and flexible substrates deposition [1, 2]. These blends has high benefit and interest in the field of organic photovoltaics and describes the optical properties for a number of potential applications [3–8]. Measurements of optical characteristics have long been regarded as an effective method for studying the electronic composition of solids. It is crucial to thoroughly examine their optical properties for the design and development of heterostructure semiconductor devices [9].

To improve the power conversion efficiency of bulk heterojunction optical sensors, a number of techniques have been proposed. One of these techniques involves mixing an electron acceptor like [6,6]-phenyl-C61-butyric acid methyl ester (PCBM) with an electron donor like poly(3-hexylthiophene) (P3HT) [10–14]. Bulk heterojunction organic optical sensors based on P3HT:PCBM have been improved in several ways, including heat, vapour, solvent, and annealing treatments, which could result in a high power conversion efficiency of more than 4% [9–12, 15, 16]. However, for two reasons, the performance of organic optical sensors based on P3HT:PCBM is still constrained. First, the bandgap of P3HT is relatively large (around 1.9 eV), which reduces sensor light harvest. The second factor has to do with the open circuit voltage (V_{oc}), which is modest (around 0.6 V) since there is only a slight energy difference between the HOMO of P3HT and the LUMO of PCBM [17]. One important material that is being explored as a nanofiller for improving polymer properties is Graphene [6, 18, 19]. It's a miracle material with exceptional physical and chemical properties, and the low density and high aspect ratio make it ideal for composite materials [20]. Enhancing composite properties requires controlling the size, shape, and surface chemistry of the reinforcement filler, resulting in homogeneous dispersion and strong interfacial interactions [21]. The use of graphene as a filler or surface layer for organic thermoelectric materials has recently attracted a lot of attention [6]. The addition of graphene to polymers significantly improves the electrical conductivity while maintaining essentially constant thermal conductivity between the composite and the polymer regardless of the addition of graphene [22, 23].

The novelty of the present work is optimization the photo-electrical properties of P3HT:PCBM active layer using Schiffbase as dopant material to fabricate organic photo-sensors on interdigitated ITO substrate. A new perspective on the electrical and photoelectrical characteristics of pure P3HT:PCBM and P3HT:PCBM:schiffbase thin films is offered in this work. At room temperature, the current–voltage characteristics of the doped/undoped P3HT:PCBM thin films were measured under dark conditions. The effects of light intensity on the photo-electrical properties were also investigated over intensity range from 0 to 50 mW cm⁻². The photo-responsivity, quantum efficiency, and reproducibility of the photo-sensors based on doped/undoped thin films were

evaluated using three different wavelengths, white, green, and red. The photo-sensors exhibit highly repeatable characteristics and a quick photo-response to light exposure. In comparison with pure P3HT:PCBM, the P3HT:PCBM:schiffbase samples have a strong optical response. The samples' optical response is lowest when exposed to red-light, while it is maximum when exposed to white-light. Additionally, the electrical and photo-electrical properties of the doped/undoped P3HT:PCBM active layer were significantly improved by depositing a carbon nano-sheet on the top of the active layer.

2. Experimental

2.1. Materials and instrumentation

4-Nitro-o-phenylenediamine and furfural were supplied from Aldrich. These chemicals were used without further purification except furfural was distilled before using in the reaction. All solvents were of analytical grade. Organic semiconductor materials, PCBM and P3HT are purchased from Osilla. Chloroform and dimethylformamide (DMF) solvents are purchased from Merck. Pre-patterned ITO substrates were purchased from Osilla.

2.2. Instruments and measurement systems

2.2.1. NMR spectroscopy. NMR technique give an important information about each atom in the molecule according to the environments and bonding between atoms through positions, numbers and integrations of the peaks as as images in the NMR spectrum. NMR spectrum of the Schiff base material was recorded on a inova spectrometer operating at 400.99 (¹H) and 125.57 MHz (¹³C) at ambient temperature.

2.2.2. FTIR spectroscopy. FTIR technique is a technique used to measure the interaction of infrared radiation with material by absorption, emission, or reflection to study and identify chemical substances or functional groups in the molecule structure. The IR spectrum of the Schiff base was obtained using the FT-IR-84005-SHIMADZU spectrophotometer with potassium bromide as a disc.

2.2.3. Mass spectrometry. Mass spectrometry technique is an analytical method that measures the mass-to-charge ratio of one or more molecules present in the sample. The electrospray ionization (ESI) mass spectrum of the Schiff base material was recorded with MeCN using Waters Alliance 2695 HPLC-Micromass Quattro micro API Mass Spectrometer.

2.2.4. Thermo scientific instrument. To measure the melting point of the Schiff base, thermo scientific instrument was used in the present work.

2.2.5. SEM measurements. To investigate the morphology of the fabricated doped/undoped P3HT:PCBM thin films

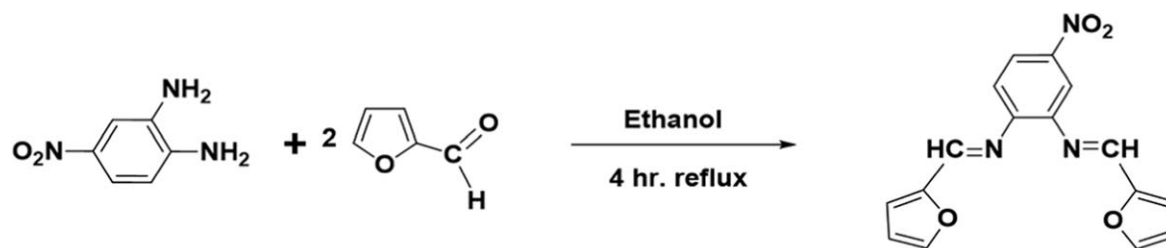


Figure 1. Scheme reaction of Schiff base material.

deposited on glass substrates, the scan electron microscopy (SEM) images of all samples were recorded using FEI Nova NanoSEM 450.

2.2.6. UV-vis spectroscopy. The spectra of the absorption and transmittance of the fabricated thin films deposited on glass substrates were carried out using UV-vis spectrophotometer double beam CE Shimadzu model 1900 i.

2.2.7. Electrical and photo-electrical measurements. To measure the current-voltage characteristics of the fabricated thin films on interdigitated ITO substrates were measured using Keithley meter (2400). Photo-sensing measurements were investigated by measuring the current-time characteristics using the system which is shown in the previous work [24].

2.3. Synthesis of Schiff-base

A hot solution of 4-Nitro-*o*-phenylenediamine (0.92 gm., 6 mmol) and 75 ml EtOH was added drop wise during 30 min to ethanolic solution (25 ml) of furfuraldehyde (1.15 g, 12 mmol) and 1 ml glacial acetic acid in a dry two-neck 250 ml round flask contains a magnetic stirrer bar. The reaction mixture was followed by refluxing for 4 h. The reaction mixture was then cooled to room temperature and the solvent was evaporated by rotary evaporation. The crude product then was purified by washing with hot di ethyl ether (3×20 ml) to give (0.56 g, 60%) as brown/red crystals, M.P. 189–190 °C. ^1H NMR (500 MHz, DMSO- d_6) (Supplementary material figure S1): δ), 6.78 (2H Furan), 7.35 (m, 1H Ar-H, 1H Furan), 8.12–8.03 (m, 2H Ar-H, 2H CH=N), ^{13}C {1H} NMR (125 MHz, DMSO- d_6): The ^{13}C NMR spectra (Supplementary material figure S2) show the expected number of signals δ 108.4, 109.6, 111.1, 113.2, 118.6, 118.9, 143.2, 144.0, 144.9, 146.4, 149.7. FT-IR (KBr) (Supplementary material figure S3): ν_{max} cm^{-1} 3124 (Ar C-H), 1629 (C=N), 1342 (C-O-C), MS-ESI m/z 311.0 [L + 2H] $^+$ $\text{C}_{16}\text{H}_{13}\text{N}_3\text{O}_4$ (Supplementary material figure S4). Schiff base derived from furfural and 4-Nitro-*o*-phenylenediamine was prepared according to the scheme reaction illustrated in figure 1.

Schiff base structure confirmed using spectrophotometry techniques. ^1H NMR spectrum shows signal at 8.03 ppm due to 2H in azomethine groups (2CH=N) as well as expected protons signals due to aromatic and furan ring protons. ^{13}C NMR spectrum shows the expected number of carbons signals and the azomethine and C-NO₂ carbons appear at at δ

146.4 and 149.7 respectively. The FT-IR spectrum shows a band at 1629 cm^{-1} due to ν_{max} (C=N) stretching without any evidence to frequency around the region 1750 cm^{-1} due to ν_{max} (C=O) stretching frequency. Furthermore, MS-ESI m/z 311.0 gives good confirmation to form Schiff base structure.

2.4. Preparation of doped/undoped P3HT:PCBM thin films

The preparation steps to fabricated the pure P3HT:PCBM and P3HT:PCBM:Schiffbase (4 mM) thin films were illustrated in figure 2. As known, the P3HT and PCBM are highly soluble in chloroform solvent, while the prepared Schiff base is highly soluble in DMF solvent but poorly soluble in chloroform. Experimentally, mixing the Schiff base solution (dissolved in DMF) with the p3HT:PCBM solution (dissolved in chloroform) together leads to the aggregation of the solution. Consequently, to overcome this problem, the 0.1 g of prepared Schiff base was firstly dissolved in 5 ml of DMF solvent under stirrer for two hours and then we add 45 ml of chloroform (the typical ratio is 1:9) to the solution of Schiff base under stirrer for 5 h. On the other hand, the solution of P3HT:PCBM was prepared as follows, 0.22 g of P3HT and 0.18 g of PCBM were dissolved in 10 ml of chloroform under stirrer for 30 min at 50 °C and then the solution left under stirrer overnight at room-temperature. Finally, 2 ml of P3HT:PCBM was mixed with 2 ml of Schiff base solution under stirrer for 6 h at room-temperature.

To fabricate the P3HT:PCBM:Schiffbase (2 mM) thin films, the weight of ligand material (Schiff-base) in step 4 was 0.05 g. All solution samples were filtered using 0.45 μm filter. After thin films fabrication, the samples annealed into oven at 140 °C for 8 min. For studying the linear optical properties, doped/undoped P3HT:PCBM thin films were deposited onto glass substrates with dimension of 2.5 cm \times 2.5 cm. To evaluate the electrical and photo-electrical properties of the thin films, ITO interdigitated electrodes was used as a substrate (see figure 3). For such electrodes, the electrical conductivity (σ) could be determined from the following formula [25]:

$$\sigma = \frac{I}{V} \frac{d}{Ltq} \quad (1)$$

Where d is the distance between the fingers electrodes, L is the length of finger, q is the number of fingers, t is the thickness of thin films. I and V are the electrical current and voltage, respectively.

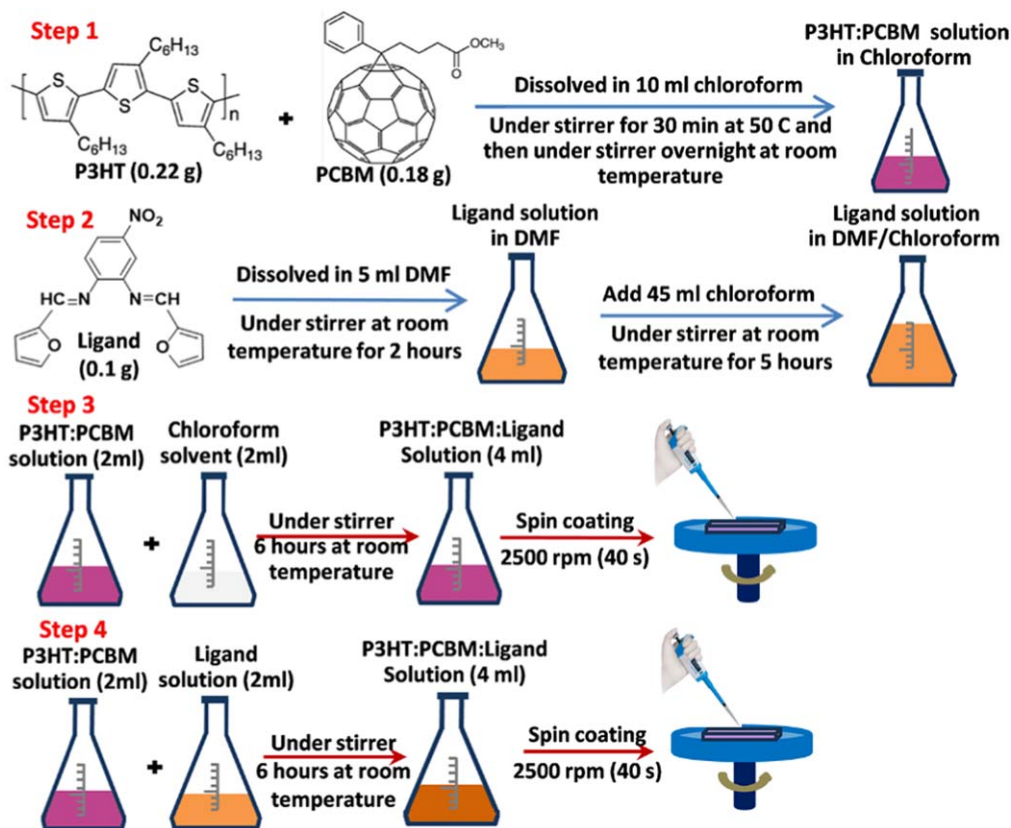


Figure 2. Schematic diagram of the preparation steps of doped/undoped P3HT:PCBM active layer.

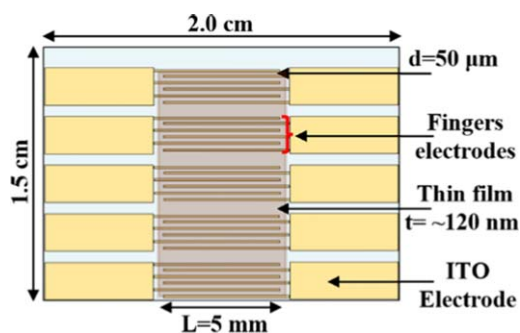


Figure 3. Pre-patterned ITO sensing substrate.

PCBM) leads to increase the absorbance. The transmission of the thin films was demonstrated in figure 4(a2), exhibiting a high transparent for wavelengths > 600 nm.

Furthermore, the absorption coefficient α was determined from the following formula [26]:

$$\alpha = 2.303 \frac{A}{t} \tag{2}$$

The results plotted in figure 4(a3), show that the values of α are greater than 10^4 , confirming that the transition is direct allowed. Therefore, to evaluate the optical gap energy E_g , $(\alpha h\nu)^2$ was plotted as a function of photon energy ($h\nu$) according to the following relation [27]:

$$(\alpha h\nu)^2 = B(h\nu - E_g) \tag{3}$$

where B is a constant, h is Planck's constant, and ν is the frequency of incident light on the film. As can be observed from figure 4(a4), the optical gap energy of the active region P3HT:PCBM slightly decreases when the dopant concentration increases, where the E_g value of the Pure P3HT:PCBM, P3HT:PCBM:Schiffbase (2 mM), and P3HT:PCBM:Schiffbase (4 mM) thin films are 2.08, 2.06, and 2.05 eV, respectively. The Schiff-base structure contains an auxochrome group (NO_2), which leads to a red-shift in the absorption peak, indicating a longer wavelength and lower energy [28]. For more in-depth discussion, one of the strong electron-withdrawing groups in the Schiff base dopant is the ($-\text{NO}_2$) group. This group promotes efficient charge transfer interactions inside the active layer by improving the Schiff base

3. Results and discussions

3.1. Optical properties of the doped/undoped P3HT:PCBM thin films

The absorbance (A) and transmission (T) spectra of the thin films deposited on glass substrate were measured as a function of wavelength over the range from 300 to 900 nm using a double beam UV-vis-NIR spectrophotometer. As illustrated in figure 4(a1), the absorbance spectrum of all thin films show broad absorption spectra with an absorbance peak at ~ 330 nm, because of the absorbance of PCBM, and a broad peak at around 500 nm due to the absorbance contribution of P3HT and PCBM with two shoulders at ~ 550 nm and ~ 600 nm due to the absorption of P3HT. It was also seen that adding Schiff base dopant to pure active region (P3HT:

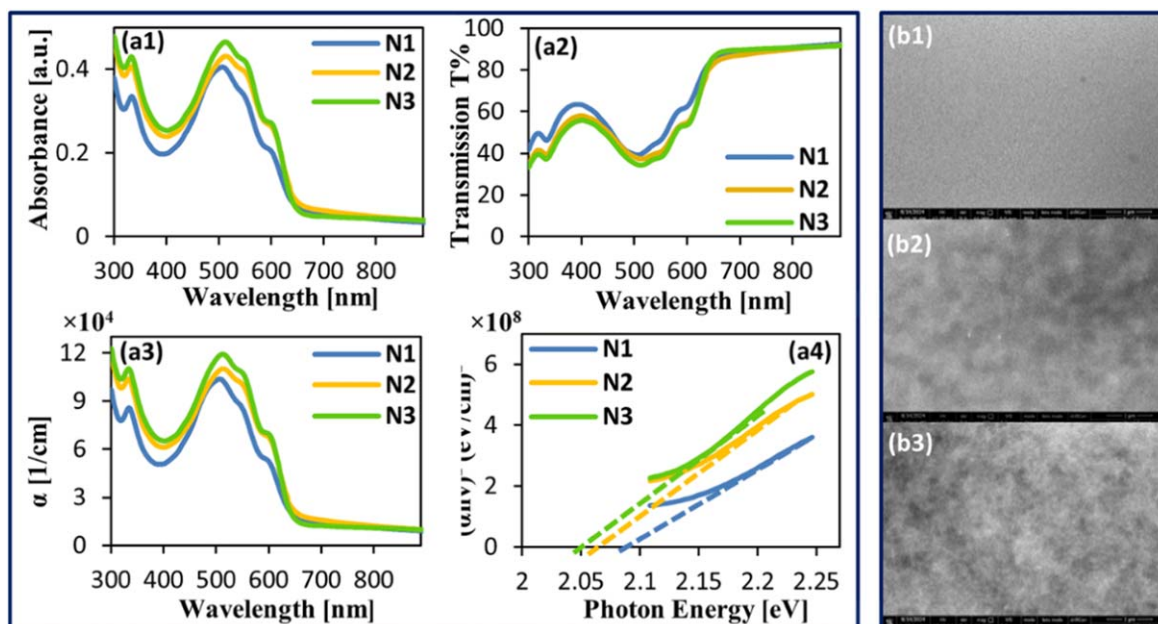


Figure 4. (a1) Absorbance spectrum, (a2) Transmission spectrum, (a3) Absorption coefficient, and (a4) The optical energy gap for pure P3HT:PCBM (N1), P3HT:PCBM:Schiffbase 2 mM (N2), and P3HT:PCBM:Schiffbase 4 mM (N3). (b1-b3) the SEM images of the samples N1, N2, and N3, respectively.

molecule's total electron removal. The Schiff base interacts with P3HT and PCBM at the molecular level through dipole–dipole and π - π stacking when it is added to the P3HT:PCBM. These interactions encourage high energy levels and strong electronic coupling with the dopant as donor. P3HT and its acceptor, PCBM, are in agreement with one another. The presence of the NO_2 group in the Schiff base system induces a red shift in the absorption spectrum, evidenced by a wider absorption and a minor reduction in the optical gap energy (E_g). This redshift results from enhanced conjugation within the active layer. In the absorption peak enhancing the effective displacement The red-shift and reduction in E_g further confirms the role of the dopant play in enhancing the optical absorption and extending the photoactive range of the material.

The morphology of the sample surfaces was examined using SEM technique, as shown in figures 4(b1)–(b3). The SEM image of the pure P3HT:PCBM active layer revealed the presence of overlapping polymer chains and a uniformly smooth surface, as depicted in figure 4(b1). The surface morphology of the P3HT:PCBM:schiffbase thin films reveal a distinct enhancement in the visibility of polymer-chain overlapping, as well as a less smooth surface in the doped thin films compared to the pure active layer.

3.2. Electrical characteristics of the doped/undoped P3HT:PCBM thin films

Figure 5 shows the room temperature current–voltage (I-V) characteristics of the doped and undoped P3HT:PCBM thin films under dark conditions. It is clearly seen that, over the voltage range 0–10 V, the characteristic curves present an ohmic behavior, where the current linearly increases with increasing the voltage. At applied voltage 10 V, the current

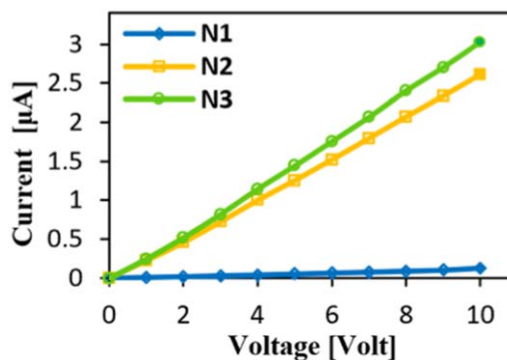


Figure 5. Current–Voltage (I-V) characteristics of pure P3HT:PCBM (N1), P3HT:PCBM:Schiffbase 2 mM (N2), and P3HT:PCBM:Schiffbase 4 mM (N3) under dark conditions.

value of the pure P3HT:PCBM thin film is about $0.13 \mu\text{A}$. This value is increased for the P3HT:PCBM:Schiffbase thin films, where their current values are about $2.6 \mu\text{A}$ and $3.0 \mu\text{A}$, at concentrations of 2 mM and 4 mM, respectively. These results exhibit that the current of pure P3HT:PCBM thin film was enhanced by factor of 20x and 24x due to doping by 2 mM and 4 mM of Schiff-base material, respectively. It is obvious that the doping of the P3HT:PCBM film at a certain concentration can have a major effect on its electrical properties and could lead to a significant improvement in its characteristic behavior. The increase in the electrical current of the doped films is owing to enhancement in concentration of charge carrier as a result of improving in the charge transfer processes. The change in concentration of the doping material can be considered a good control parameter for the electrical behavior of the blend polymer.

Figure 6 illustrates the photo-electrical characteristics of the doped and undoped P3HT:PCBM thin films at room

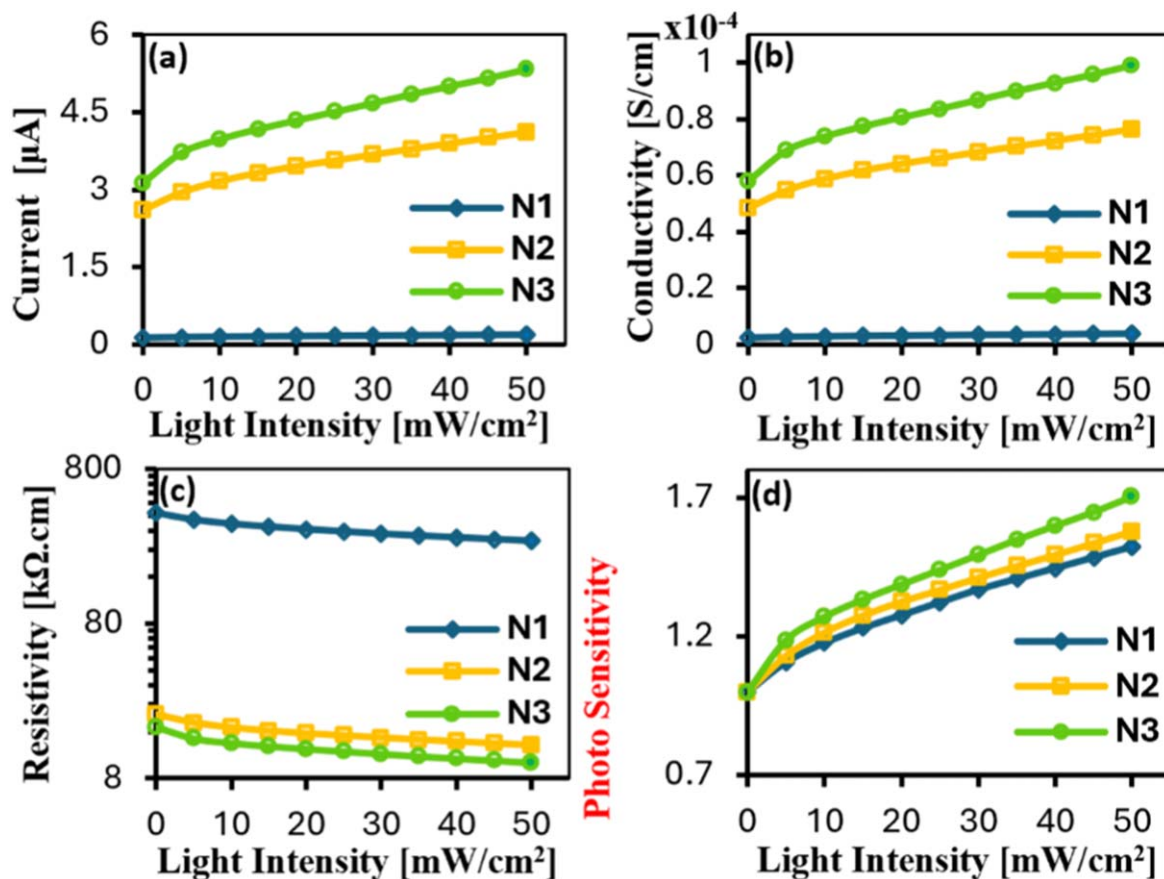


Figure 6. (a) Electrical current, (b) Electrical conductivity and (c) Electrical resistivity and (d) Photo-sensitivity as a function of light intensity for doped/undoped P3HT:PCBM thin films.

temperature. The photo-current, photo-conductivity (σ), photo-resistivity (ρ), and photo-sensitivity (S_{ph}) of the thin films are plotted as a function of light intensity (I_0) over the intensity range 0–50 mW cm^{-2} at applied voltage 10 V. To illuminate the samples, a white light of adjustable light intensity was used as a source light. As seen in figure 6(a), the photo-current of the fabricated thin films, starts to increase with increasing the light intensity. Under 50 mW cm^{-2} illumination, the photo-current obtained from P3HT:PCBM: Schiffbase 2 mM (N2) and P3HT:PCBM:Schiffbase 4 mM (N3) thin films are $\sim 4.1 \mu\text{A}$ and $\sim 5.3 \mu\text{A}$, respectively. It is clearly noticed that these values are higher than that of the pure P3HT:PCBM film (N1) by a factor of $\sim 21.5x$ and $\sim 27x$, respectively, where the current of the pure thin film was about 0.2 μA . The enhancement in the photo-current is attributed to increase the mobility as a result of photo-induced charge transfer process and generate the excitons by photo-excitation process [1].

One of the most important electrical parameters is the electrical conductivity of the material. Figure 6(b) represents the results of this parameter for the prepared thin films. As the light intensity increases from 0 to 50 mW cm^{-2} , the conductivity of the undoped P3HT:PCBM thin film increase from 0.024×10^{-4} to 0.037×10^{-4} S cm^{-1} . Doping of P3HT:PCBM active layer leads to enhance the conductivity of the P3HT:PCBM:Schiffbase thin films at dopant concentration of

2 mM and 4 mM, where the conductivity of these two samples increases from 0.48×10^{-4} S cm^{-1} and 0.58×10^{-4} S cm^{-1} at dark state to about 0.76×10^{-4} S cm^{-1} and 1.0×10^{-4} S cm^{-1} at illumination of 50 mW cm^{-2} , respectively. The electrical resistivity shows the opposite behavior of conductivity as demonstrated in figure 6(c), where the resistivity of the thin films decreases when light intensity increases. The results exhibit that the resistivity of the undoped P3HT:PCBM thin film, at dark conditions, begins at 415 $\text{k}\Omega\cdot\text{cm}$ and gradually starts to drop as the light intensity increases until it reaches about 273 $\text{k}\Omega\cdot\text{cm}$ at illumination of 50 mW cm^{-2} . The resistivity of P3HT:PCBM:Schiffbase films at the two concentrations, 2 mM and 4 mM, exhibits an appreciable drop to the lowest values, about 13 $\text{k}\Omega\cdot\text{cm}$ and 10 $\text{k}\Omega\cdot\text{cm}$, at a light intensity of 50 mW cm^{-2} , confirming that the photo-resistivity of the doped thin films are lower than the corresponding value of the pure thin film.

Figure 6(d) illustrates the photo-sensitivity characteristics of the optical sensor as a function of the light intensity. It is clearly observed that the prepared thin films are exhibiting good photo-sensing to the incident light. The photo-sensitivity is a light intensity dependence; it increases with increasing the light intensity. Increasing the concentration of the P3HT:PCBM:Schiffbase film sample is also leading to an important development in the photo-sensitivity of the thin films, where this parameter increase with increasing the

Table 1. The current (I), conductivity (σ), and photo-sensitivity (S_{ph}) of the fabricated thin films, under dark and illumination conditions at applied voltage of 10 V, including some results reported in the literatures.

Sample	Under dark condition		Under illumination condition (50 mW cm ⁻²)		S_{ph}
	I (μ A)	σ (S/cm) $\times 10^{-4}$	I (μ A)	σ (S/cm) $\times 10^{-4}$	
Pure P3HT:PCBM	0.13	0.024	0.2	0.037	52%
P3HT:PCBM:Schiffbase (2 mM)	2.6	0.483	4.1	0.763	60%
P3HT:PCBM:Schiffbase (4 mM)	3.0	0.581	5.3	0.989	70%
	Present work				
P3HT:PCBM/C N-Sh	1.64	0.303	3.0	0.555	84%
P3HT:PCBM:Schiffbase (2 mM)/ C N-Sh	19.28	3.57	36.29	6.72	88%
P3HT:PCBM NPs [6]	2.15	~ 0.355	0.37	~ 0.57	
P3HT:CrCl ₂ (10 wt%) [24]	~ 10.2	~ 1.427	~ 34	~ 5.75	
P3HT:PbI ₂ [33]	—	1.0	—	—	

concentration of the doped thin films from 60% at 2 mM to 70% at 4 mM.

The photo-sensing mechanism could be explained as follows: An exciton is produced when light illuminates the P3HT, causing electrons to move from the HOMO to the LUMO. The P3HT is suitable for electron donation because of its HOMO energy level of about -5.2 eV. Conversely, a PCBM, that has a LUMO energy level of approximately -4.0 eV, is an effective electron acceptor. However, the energy difference between the LUMOs of P3HT and PCBM led to ultrafast electron transfer from P3HT to PCBM. This charge transfer from the donor to acceptor is ultrafast and efficiently results in free charge carriers [29]. This mechanism correctly separates the electrons from the holes, leaving the holes out of the P3HT and the electrons trapped within the PCBM. Once separated, the electrons are transferred from the PCBM to the cathode electrode and the holes are transferred through the P3HT to the anode electrode, generating an electric current in response to incident light. In the other hand, the presence of nitro groups can enhance the charge transfer properties at interface between P3HT and PCBM. It can form localized dipoles that facilitate efficient separation of electron-hole pairs, thereby increasing the photocurrent.

Table 1 summarizes the measured values of the electrical current (I) and electrical conductivity (σ) of the prepared doped/undoped P3HT:PCBM thin films under the two conditions, dark and the light illumination, at applied voltage 10 V. The results exhibit that the electrical parameters, σ , ρ , and S_{ph} , of the thin films under illumination are higher than those under dark due to enhancement in the photo-current as a result of generate the electron-hole pairs by photo-excitation process. Furthermore, this table show that the doping of the blend P3HT:PCBM by Schiff-base is leading to a significant improvement in the electrical properties of this blend polymer. The unique structural features of the Schiff-base arise from its composition, which includes oxygen and nitrogen heteroatoms as donor atoms, a π -spacer in the form of $-\text{CH}=\text{N}-$, and a delocalized conjugated π -system in the aromatic system. The significantly enhanced electrical properties of P3HT:PCBM:Schiff-based thin films can be also

attributed to the addition of NO_2 group in Schiff-based molecules NO_2 group, as an electron-withdrawing substituent, plays an important role in molecular charge promoting transfer and increasing overall charge transport properties. Tahir *et al* [28] reported that electron-withdrawing groups such as NO_2 enhance π -conjugation and electron displacement in molecular systems, thereby improving charge-transfer processes. Similarly, Irfan *et al* [30] demonstrated that the NO_2 group enhances intramolecular charge transfer mechanisms by increasing the π electrons in the Schiff base structures, thereby improving the charge carrier mobility. The role of the NO_2 group in Schiff base molecules in our experiments with P3HT:PCBM matrix. It is evident in the ability to improve interactions. Greatly improved conductance measurements now show how this interaction increases the number of charge carriers. The NO_2 group favored π conjugation in Schiff base molecules provides effective means to realize charge hopping and charge recombination reduction, which significantly increase electrical conductivity and reduce resistance, especially in the presence of light with the base compounds the observed behaviors are consistent.

In order to examine the stability and the reproducibility of the organic photo-sensor based on doped/undoped P3HT:PCBM thin films, the time-dependent electrical properties of these devices were investigated at applied voltage 10 V as illustrated in figure 7. Three light sources of different wavelengths, white-light, green-light, and red-light, were used to illuminate the photo-sensors with intensity of 50 mW cm^{-2} . The electrical current, conductivity, and resistivity of the photo-sensors were measured over the time range 0–1200 s, 120 s into light followed by 120 s into dark, at room temperature. It is clearly noticed in figure 7, that the photo-sensors exhibit good photo-response and repeatability in the pulse mode. The electrical parameters of the samples exhibited pulse-shaping behaviors with time, where the values of these parameters sharply grow up to saturation when the light is switched on and then start to drop down when the light is switched off. The pulse starts to recover, and the behavior is repeated as the time continues to increase.

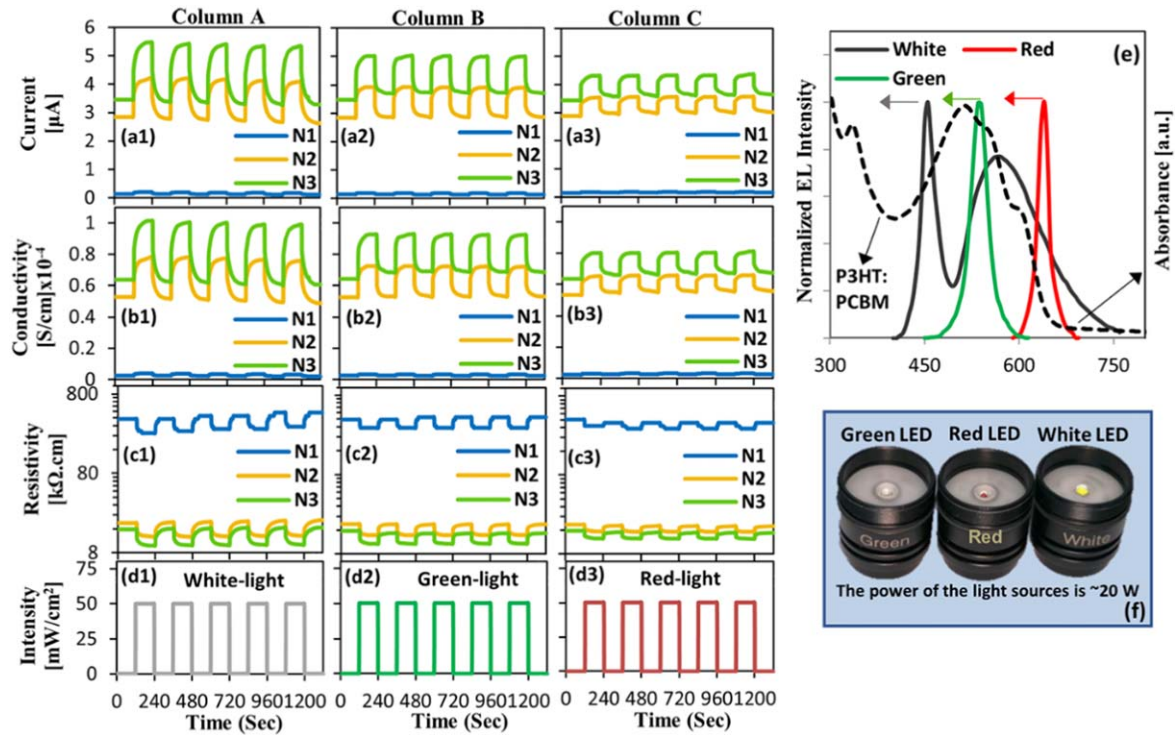


Figure 7. (a1)–(a3) Electrical current, (b1)–(b3) Electrical conductivity and (c1)–(c3) Electrical Resistivity (log scale) as a function of time for pure P3HT:PCBM (N1), P3HT:PCBM:Schiffbase 2 mM (N2), and P3HT:PCBM:Schiffbase 4 mM (N3) under light intensity of 50 mW cm^{-2} (white-light (column A), green-light (column B), and red-light (column C)). (d1)–(d3) the light intensity of the light sources as a function of time. (e) the emission spectra of the LEDs and the absorbance spectrum of the active layer of the fabricated samples. (f) Light sources.

It was also found from figure 7 that the electrical parameters, current, conductivity, and resistivity, of the photo-sensors are significantly improved due to doping by Schiff-base material. Furthermore, it is observed that the values of the electrical parameters of the photo-sensors are clearly wavelength dependent, where the highest values of these parameters were obtained when the samples illuminated by white light (see figure 7 column A) and the smallest values were recorded when the samples exposed by red light (see figure 7 column C). In order to obtain an interpretation for the dependence of these parameters on the light wavelength, the emission spectra of the light sources and the absorption spectrum of the active layer of the samples have been plotted in figure 7(e). When the white-light emission spectrum compares with those of the other light sources, we find that the white light spectrum exhibits a high overlapping with the absorption spectrum of the active layer. This confirms that the number of absorbed photons by the active layer is higher than that for the other light sources. Thus, the number of excitons generated in the samples exposed by white-light is greater than that in the samples exposed by other two light-sources (the green and red). On the other hand, the overlapping between the red-light emission spectrum and the absorption spectrum of the active layer is very low, indicating that the number of the absorbed photons by the active layer is very low. In addition, the photon energy of the red light is relatively less than that for both the white and green light. Consequently, the number of excitons generated by illuminating

the active layers with red-light is also very low. This explains why the performance of the photo-sensors under red-light exposure is very poor.

Based on the time-dependent electrical current results, the photo-responsivity (R_{ph}) and the quantum efficiency (η) of the photo-sensors were determined using the following formulas [31, 32]:

$$R_{ph} = \frac{I_{illum} - I_{dark}}{AI_0} \quad (4)$$

and

$$\eta = \frac{hc}{e\lambda} R_{ph} \quad (5)$$

where A is the exposed area of the photo-sensor, c is the light velocity, I_0 is the light intensity, h is Planck's constant, e is the electron charge, and λ is the wavelength of incident light. The results show that R_{ph} and η values of the photo-sensors are also wavelength-dependent, and significantly improved due to doping the active layer (pure P3HT:PCBM) by the Schiff-base material (see table 2).

3.3. Photo-electrical properties of the doped/undoped P3HT:PCBM/carbon nano-sheet thin films

In order to optimize the optical and photo-electrical properties of the doped/undoped P3HT:PCBM active layers, a carbon nano-sheet ($4.8 \text{ nm} \pm 0.2 \text{ nm}$) was deposited on the top of these layers using sputtering technique. As can be seen in

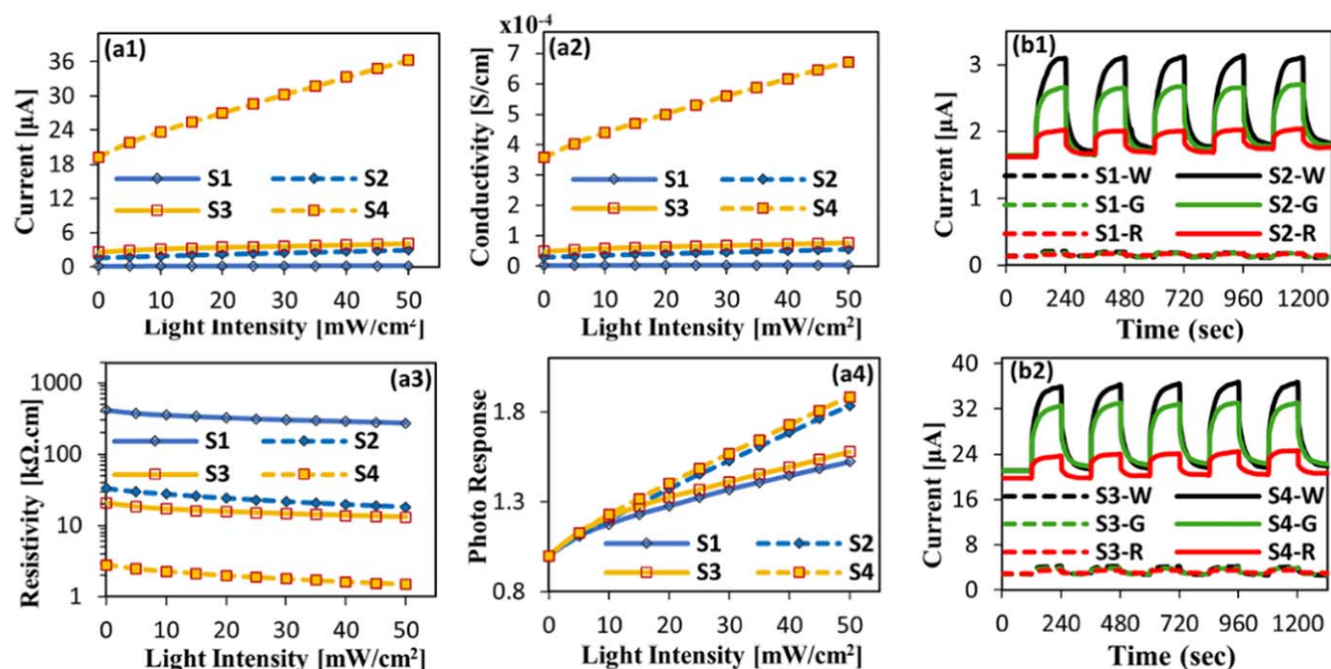


Figure 8. (a1) Photo-current, (a2) Electrical conductivity, (a3) Electrical resistivity, (a4) Photo-sensitivity as a function of light intensity, (b1) and (b2) Photo-current as a function of time for pure P3HT:PCBM (S1), P3HT:PCBM/Carbon nano-sheet (S2), P3HT:PCBM:Schiffbase 2 mM (S3), and P3HT:PCBM:Schiffbase 2 mM Carbon⁻¹ nano-sheet (S4). The base voltage is 10 V.

Table 2. The photo-sensitivity (S_{ph}), photo-responsivity (R_{ph}), and efficiency (η) of the photo-sensors at applied voltage of 10 V for three different wavelength, white, green, red, including some results reported in the literatures.

Sample	λ	S_{ph}	R_{ph} (mA/W)	η
P3HT:PCBM	White	46%	0.105	0.026%
P3HT:PCBM:Schiffbase 2 mM		54%	2.38	0.6%
P3HT:PCBM:Schiffbase 4 mM		62%	3.32	0.82%
P3HT:PCBM/C nano-sheet		68%	1.70	0.42%
P3HT:PCBM:Schiffbase(2 mM)/C nano-sheet	Green	86%	23.9	6%
P3HT:PCBM		36%	0.078	0.018%
P3HT:PCBM:Schiffbase 2 mM		37%	1.72	0.4%
P3HT:PCBM:Schiffbase 4 mM		37%	2.22	0.52%
P3HT:PCBM/C nano-sheet	Red	65%	1.30	0.3%
P3HT:PCBM:Schiffbase(2 mM)/C nano-sheet		49%	17.6	4.1%
P3HT:PCBM		18%	0.043	0.008%
P3HT:PCBM:Schiffbase 2 mM		19%	0.905	0.17%
P3HT:PCBM:Schiffbase 4 mM	20%	1.17	0.22%	
P3HT:PCBM/C nano-sheet	18.5%	0.58	0.1%	
P3HT:PCBM:Schiffbase(2 mM)/C nano-sheet	19%	6.4	1.2%	
P3HT:AuNPs (Photo diode) [34]	Solar simulator	—	0.3356	—
P3HT:CrCl ₂ (10 wt%) (Photo-sensor) [24]	White	~71%	23.26	~5.77
NPD:Alq ₃ (Photo-diode) [35]	UV	1.3×10^5	5.39	—
TPD:Alq ₃ (Photo-diode) [36]	UV	1.76×10^5	0.522	—
P3HT:VOPcPhO (Photo-diode) [37]	Solar simulator	—	0.21	—

(Supplementary material figure S5), the absorbance spectra of the pure P3HT:PCBM and P3HT:PCBM:Schiffbase(2 mM) thin films with carbon nano-sheet are higher than those of the thin films without carbon nano-sheet.

The photo-electrical properties of the thin films based on P3HT:PCBM/Carbon nano-sheet (S2) and P3HT:PCBM:Schiffbase(2 mM)/carbon nano-sheet (S4) were investigated and

plotted in figure 8. The photo-electrical parameters, the current, conductivity, resistivity, and sensitivity were carried out using white light source with intensity varying from 0 to 50 mW cm⁻² at applied voltage of 10 V as shown in figures 8(a1)–(a4). As can be noticed from this figures, the photo-electrical parameters of these two samples are highly enhanced due to deposit the carbon nano-sheet on the top of the their active layers. The

values of these parameters were listed in table 1, showing that the electrical current, conductivity, and resistivity of the thin film based on pure P3HT:PCBM/carbon nano-sheet are greater than those the corresponding values of the thin film without carbon nano-sheet by a factor of 12.5x at dark state and by a factor of 14.5x at light intensity of 50 mW cm^{-2} . For the thin film based on P3HT:PCBM:Schiffbase(2 mM)/carbon nano-sheet, the results show that these parameters are also enhanced by a factor of 7.5x under dark and by a factor of 9x under light intensity of 50 mW cm^{-2} . It was also found from figure 8(a4), the photo-sensitivity of the samples S2 and S4 are evaluated and determined to be $\sim 84\%$ and $\sim 88\%$, respectively. The enhancement in the electrical and photo-electrical parameters of the thin films/carbon nano-sheet is could be attributed to the optimizing of the effective mobility and the charge carrier transport as a result of depositing the carbon nano-sheet on the top of the active layer.

At room temperature, the electrical characteristics of the photo-sensors were investigated as a function of time varying from 0 to 1200 s and under three different light wavelengths, white, green, and red. The results exhibit that the photo-sensors have a very good reproducibility and fast optical response as demonstrated in figures 8(b1) and (b2). In comparison, the photo-responsivity (R_{ph}), photo-sensitivity (S_{ph}), and quantum efficiency (η) of the photo-sensors based on doped/undoped P3HT:PCBM/carbon nano-sheet thin films is higher than those the corresponding values of the photo-sensors without carbon nano-sheet. Furthermore, the findings revealed that the photo-electrical parameters of the organic photo-sensors are wavelength dependent as listed in table 2, where the values of these parameters of the sensors exposed by white light are higher than those values measured under green light, while the smallest values were recorded under red light. The values of R_{ph} and η of the P3HT:PCBM/carbon nano-sheet based photo-sensor were evaluated and their values are $\sim 1.76 \text{ mA W}^{-1}$ and $\sim 0.43\%$, respectively, showing an enhancement by a factor of about 17x compared to corresponding values of the sensor without carbon nano-sheet. The highest values of R_{ph} and η were recorded from the photo-sensor based on P3HT:PCBM:Schiffbase(2 mM)/carbon nano-sheet active layer under white light illumination, where the values of these two parameters are $\sim 23.9 \text{ mA W}^{-1}$ and $\sim 6\%$, respectively, exhibiting an improvement by a factor of $\sim 10x$ compared to those the corresponding values of the sensor without nano-sheet.

The carbon nano-sheet, characterized by its good conductivity and wide surface area, acts as an effective charge transport layer. When applied to the active layer (P3HT:PCBM:Schiff base), it enhances charge removal and reduces recombination losses at the interface. This is especially important in doped layers, where the Schiff bases are stable sites for charge carrier generation. The incorporation of the Schiff base into the P3HT:PCBM matrix changes the relative energy level of the active layer. The carbon nano-sheet provides an additional interface with an advantageous energy layer that enhances the effect of the Schiff base. This alignment assures efficient charge injection and extraction, thereby enhancing the photoelectric properties. The carbon nano-sheet Schiff stabilizes the charge carriers produced in the base-doped active layer. The conductive network of the nano-sheet

facilitates efficient carrier movement, reducing the probability of capture and recombination. This enhances the performance metrics seen in different lighting conditions.

4. Conclusions

The obtained results of the electrical properties of the doped/undoped P3HT:PCBM thin films revealed an indication that the prepared P3HT:PCBM:Schiffbase active layer based thin films are promising candidates for photonic device applications. The doping of the P3HT:PCBM active layer with a Schiff base material led to an excellent improvement in its electrical and photo-electrical properties. Under dark current, the current and conductivity of the P3HT:PCBM:Schiffbase (2 mM) thin films are higher than those values of the pure P3HT:PCBM thin films by a factor of 24x. This optimization in the electrical properties is attributed to increase in the concentration of charge carrier as a result of improving in the charge transfer processes. The current-illumination characteristics of thin films are also investigated, showing that the photo-current increases as light intensity increases due to increase the mobility as a result of photo-induced charge transfer process and generate the electron-hole pairs by photo-excitation process. Under light intensity of 50 mW cm^{-2} , doping of P3HT:PCBM active layer by Schiff base with concentration of 4 mM led to enhance the photo-current and photo-conductivity by $\sim 27x$. Furthermore, the photo-electrical properties of the doped/undoped P3HT:PCBM active layer based photo-sensors were evaluated as a function of time, confirming that these sensors exhibit high photo-response and very good reproducibility. It was also found that the photo-electrical parameters are wavelengths dependent, where the highest values of the photo-responsivity and quantum efficiency were obtained under white light, while the lowest values were achieved under red light. However, the electrical and photo-electrical properties of the doped/undoped P3HT:PCBM based photo-sensors are also significantly improved by depositing an ultra-thin layer of carbon on the top of the active layer, where, in comparison with pure P3HT:PCBM thin films, the current and conductivity of the pure P3HT:PCBM/carbon nano-sheet thin film are enhanced by a factor of 12.5x under dark conditions and by a factor of 15x under illumination conditions. For P3HT:PCBM:Schiffbase/carbon nano-sheet thin film, the values of current and conductivity are higher than those the corresponding values of the thin film without nano-sheet by a factor of 7.5x under dark conditions and by a factor of 9x under illumination conditions. The photo-electrical properties, photo-response and reproducibility of the photo-sensors based on doped/undoped P3HT:PCBM/carbon nano-sheets thin films are also investigated under three different wavelengths, white, green, and red. The results show that the sensors exhibit a fast photo-response with a very good reproducibility and that their performance are highly effected by the incident light wavelength. It was also found that, depositing carbon nano-sheet layer on the top of the active layer of the photo-sensors led to improve the photo-responsivity and the quantum efficiency of the samples, where, under white light, the values of these two parameters for photo-sensor based on P3HT:PCBM:Schiffbase(2 mM)/carbon nano-

sheet are enhanced by a factor of 10x and for photo-sensor based on P3HT:PCBM/carbon nano-sheet are enhanced by a factor of 16x compared with those the corresponding values of the sensors without carbon nano-sheet. The reason of the optimizing of the electrical and photo-electrical properties of the could be attributed to improve the effective mobility of the active layers. The present findings suggest applying these prepared thin films as sensitive optical sensors for the detection of light radiation.

References

- [1] Jeong J W, Huh J W, Lee J I, Chu H Y, Pak J J and Ju B K 2010 *Thin Solid Films* **518** 6343–7
- [2] Girtan M 2013 *Org. Electron.* **14** 200–5
- [3] Benchaabane A, Ben Hamed Z, Lahmar A, Sanhoury M A, Kouki F, Zellama K, Zeinert A and Bouchriha H 2016 *Appl. Phys. A* **122** 720
- [4] Kadem B, Fakher Alfahed R K, Al-Asadi A S and Badran H A 2020 *International Journal for Light and Electron Optics* **204** 164153
- [5] Mahendia P, Chauhan G, Wadhwa H, Kandhol G, Mahendia S, Srivastava R, Sinha O P, Clemons T D and Kumard S 2021 *J. Phys. Chem. Solids* **148** 109644
- [6] Tuma F A, Al-Mudhaffer M F and Al-Saymari F A 2023 *J. Nanopart. Res.* **25** 224
- [7] Amin P O, Muhammadsharif F F, Saeed S R and Ketuly K A 2022 *Opt. Quant. Electron* **54** 510
- [8] Amin P O, Muhammadsharif F F, Saeed S R and Ketuly K A 2023 *Sustainability* **15** 12442
- [9] Mardi S, Yusupov K, Martinez P M, Zakhidov A, Vomiero A and Reale A 2021 *ACS Omega* **6** 1073–82
- [10] Ma W, Yang C, Gong X, Lee K and Heeger A J 2005 *Adv. Funct. Mater.* **15** 1617–22
- [11] Li G, Shrotriya V, Huang J, Yao Y, Moriarty T, Emery K and Yang Y 2011 *Materials for Sustainable Energy: a Collection of Peer-reviewed Research and Review Articles From Nature Publishing Group, World Scientific* 80–4
- [12] Kim Y, Cook S, Tuladhar S M, Choulis S A, Nelson J, Durrant J R, Bradley D D, Giles M, McCulloch I and Ha C-S 2011 *Materials for Sustainable Energy: a Collection of Peer-reviewed Research and Review Articles From Nature Publishing Group, World Scientific* 63–9
- [13] Saidi H, Hidouri T, Amri C, Baccar H, Saidi F, Herrero B R and Bouazizi A 2020 *Adv. Nat. Sci.: Nanosci. Nanotechnol.* **11** 025011
- [14] Nguyen N D, Kim H-K, Nguyen D L, Nguyen D C and Nguyen P H N 2019 *Adv. Nat. Sci.: Nanosci. Nanotechnol.* **10** 015005
- [15] Zhao Y, Xie Z, Qu Y, Geng Y and Wang L 2007 *Appl. Phys. Lett.* **90** 043504
- [16] Wang W, Wu H, Yang C, Luo C, Zhang Y, Chen J and Cao Y 2007 *Appl. Phys. Lett.* **90** 183512
- [17] Zhao G, He Y and Li Y 2010 *Adv. Mater.* **22** 4355–8
- [18] Mahendia P, Chauhan G, Wadhwa H, Kandhol G, Mahendia S, Srivastava R, Sinha O P, Clemons T D and Kumard S 2021 *Journal of Physics and Chemistry of Solids* **148** 109644
- [19] Snyder G J and Toberer E S 2008 *Nat. Mater.* **7** 105–14
- [20] Novoselov K S, Geim A K, Morozov S V, Jiang D, Zhang Y, Dubonos S V, Grigorieva I V and Firsov A A 2004 *Science* **306** 666–9
- [21] Zhang Y, Tan Y-W, Stormer H L and Kim P 2005 *Nature* **438** 201–4
- [22] Geim A K 2009 *Science* **324** 1530–4
- [23] Liu Z, Li J, Sun Z, Tai G, Lau S and Yan F 2012 *ACS nano* **6** 810–8
- [24] Mahdi A and Al-Saymari F A 2024 *Phys. Scr.* **99** 85517
- [25] Ziadan K M, Hussein H F and Ajeel K I 2012 *Energy Procedia* **18** 157–64
- [26] Jabber W H, Hassan Q and Al-Saymari F A 2023 *Journal of Fluorescence* **33** 2369–80
- [27] Tauc J 1987 *J. Non-Cryst. Solids* **149** 97–8
- [28] Tahir M H, Mubashir T, Shah T-U-H and Mahmood A 2018 *J. Phys. Org. Chem.* 3909
- [29] Khlyabich P P, Burkhart B, Rudenko A E and Thompson B C 2013 *Polymer* **54** 5267–98
- [30] Irfan A, Al-Sehemi A G and Kalam A 2022 *Materials* **15** 8590
- [31] Mahdi M A, Hassan J J, Ahmed N M, Ng S S and Hassan Z 2013 *Superlattices Microstruct.* **54** 137–45
- [32] Li L, Wu P, Fang X, Zhai T, Dai L, Liao M, Koide Y, Wang H, Bando Y and Golberg D 2010 *Adv. Mater.* **2** 3161–5
- [33] Almohammed A, Khan M T, Benganem M, Aboud S W, Shkir M and Alfaify S 2020 *Mater. Sci. Semicond. Process.* **120** 105272
- [34] Arua P and Joseph C M 2021 *Mater. Lett.* **295** 129726
- [35] Alzahrani H, Sulaiman K, Muhammadsharif F F, Abdullah S M, Mahmoud A Y, Bahabry R R and Ab Sani S F 2021 *J. Mater. Sci., Mater. Electron.* **32** 14801–12
- [36] Basir A, Alzahrani H, Sulaiman K, Muhammadsharif F F, Abdullah S M, Mahmoud A Y, Bahabry R R, Alsoufi M S, Bawazeer T M and Ab Sani S F 2021 *Mater. Sci. Semicond. Process.* **131** 105886
- [37] Ahmed Z, Abdulla S M and Sulaiman K 2013 *Measurement* **46** 2073–6